

# Mechanical, Thermal Properties, and Flame Retardancy of PC/Ultrafine Octaphenyl-POSS Composites

Lamei Li, Xiangmei Li, Rongjie Yang

School of Material Science and Engineering, National Laboratory of Flame Retardant Materials, Engineering Research Center of Fire-Safe Materials and Technology, Ministry of Education, Beijing Institute of Technology, Beijing 100081, People's Republic of China

Received 22 April 2011; accepted 30 July 2011

DOI 10.1002/app.35443

Published online 23 November 2011 in Wiley Online Library (wileyonlinelibrary.com).

**ABSTRACT:** Composites of ultrafine polyhedral oligomeric octaphenyl silsesquioxane (OPS) and polycarbonate (PC) were prepared by melt blending. The mechanical and thermal properties of the composites were characterized by tensile and flexural tests, impact test, differential scanning calorimeter (DSC), dynamic mechanical analysis (DMA), and thermal gravimetric analysis (TGA). Rheological properties of these melts were tested by torque rheometer. The flame retardancy of the composites was tested by limiting oxygen index (LOI), the vertical burning (UL-94), and cone calorimeter test. The char residue was characterized by scanning electron microscope (SEM) and ATR-FTIR spectrum. Furthermore, the dispersion of OPS particles in the

PC matrix was evidenced by SEM. The results indicate that the glass transition temperatures ( $T_g$ ) and torque of the composites decrease with increasing OPS loading. The onset decomposition temperatures of composites are lower than that of PC. The LOI value and UL-94 rating of the PC/OPS composites increase with increasing loading of OPS. When OPS loading reaches 6 wt %, the LOI value is 33.8%, UL-94 (1.6 mm) V-0 rating is obtained, and peak heat release rate (PHRR) decreases from 570 to 292  $\text{kJ m}^{-2}$ . © 2011 Wiley Periodicals, Inc. *J Appl Polym Sci* 124: 3807–3814, 2012

**Key words:** polycarbonate; flame retardance; polyhedral oligomeric octaphenyl silsesquioxanel

## INTRODUCTION

Bisphenol A PC is an amorphous and polar commercial thermoplastic engineering plastics. Because of its outstanding comprehensive properties, such as dimensional stability, high impact strength, transparency, electrical properties, and so on, it has been widely used in the fields of building materials, auto industry, medical material, electronic, and electric equipments.<sup>1,2</sup> PC by itself shows about 26% in the LOI test and a V-2 rating in the UL-94 test. However, some applications also need more stringent flame retardant performance, such as UL-94 V-0 rating. Some halogen-containing flame retardants that have outstanding flame-retarded efficiency have been prohibited gradually due to environmental hazard. As result, some halogen-free flame retardants have been developed to meet the new regulations and standards. Several flame retardant based on silicon compounds have arisen attention owing to the

environment friendly, nontoxic, and low smoke during combustion. These silicon compounds have also shown themselves to be a perfect replacement for halogen compounds. Further, adding these silicon compounds to polymers don't adversely affect strength, moldability, and heat resistance; impact strength is better than that of polymers containing a bromine compound as a flame retardant.<sup>3–10</sup>

Polyhedral oligomeric silsesquioxanes (POSS) is a kind of organic–inorganic hybrid material. It combines the thermal stability of inorganic materials with advantage of organic materials. Recently, a few scientific papers have been published on the use of POSS as flame retardants. Moreover, the incorporation of POSS can lead to dramatic improvement of some properties such as increases in use temperature, oxidation resistance, as well as reductions in flammability and viscosity during processing.<sup>11–13</sup> The polypropylene (PP)/POSS composites have been investigated by Fina. POSS with methyl, vinyl or phenyl organic group were used to preparation of PP/POSS composites, and the POSS dispersion, mechanical properties, thermal stability, and flammability were studied. PP/vinyl-POSS composites had higher mechanical performances, HRR reduction, and slightly increased LOI value. The role of metal functionalized POSS on the combustion properties of PP composites was investigated, the results showed

Correspondence to: X. Li (bjlglxm@bit.edu.cn).

Contract grant sponsor: National High Technology Research and Development Program 863; contract grant number: 2007AA03Z538.

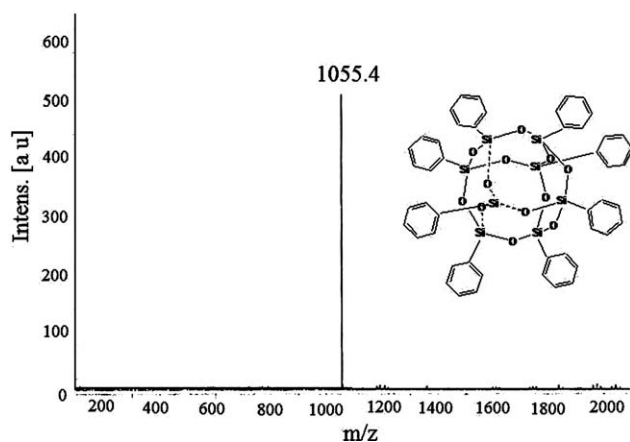


Figure 1 MALDI-TOF spectrum of OPS compound.

that Al-POSS led to a decrease of HRR (43% at 10 wt % POSS loading) with respect to neat PP due to the formation of a moderate amount of char residue, Zn-POSS did not significantly affect the PP combustion behavior. Zhou et al.<sup>14</sup> investigated the comparison of physical blending and reactive blending; he found that reactive blending composites had better mechanical properties, thermal stability, flame retardancy than physical blending composites. A few research papers have reported the thermal and combustion properties of PC / POSS composites.<sup>15–17</sup> The result showed that the addition of trisilanophenyl-POSS at 2 wt % lead to the maximum decrease of the PHRR. And the PC was a transparent sample up to 5 wt % trisilanophenyl-POSS content. Slightly enhanced mechanical properties are observed with the increase of trisilanophenyl-POSS loading.

However, comprehensive study on flame retardant polycarbonate with OPS hasn't been reported up to now, especially burn rating and LOI. In the paper, the effect of OPS on PC combustion behavior was particularly discussed, and mechanical and thermal properties of PC/OPS composites were further investigated.

## EXPERIMENTAL

### Materials

Phenyltrichlorosilane was purchased from Dalian Yuanyong Organosilicon Plant. Benzene and ethanol were from Beijing Chemical Works. Tetramethylammonium hydroxide was obtained from Beijing Institute of Fubide Fine Chemical. PC was a Makrolon 2805, purchased from Bayer Materials science.

### Synthesis of OPS

OPS has been synthesized by hydrolytic condensation of phenyltrichlorosilane in our laboratory by improved method according to previously reported

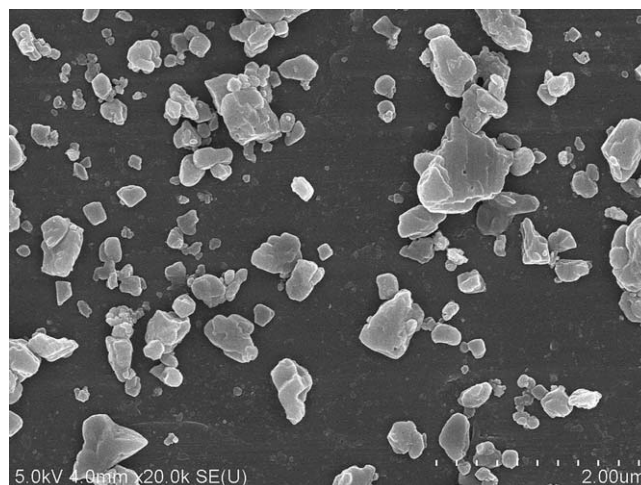


Figure 2 SEM picture of OPS particles.

literature.<sup>18–20</sup> Phenyltrichlorosilane was dissolved in 100 mL of benzene and dripped with 100 mL water for 3 h. After removing the aqueous layer, the organic layer was added with the methanol solution of tetramethylammonium hydroxide as catalyst. The mixture was heated to 85°C, and refluxed for 20 h. The product obtained was purified, using the ethanol to remove the soluble impurity, and further dried for 3 h *in vacuo* oven at 80°C to get the ultra-fine OPS to yield 97.9%. The purity was 98.4% by the ultra performance liquid chromatography (UPLC), and the MALDI-TOF result shows a single peak in 1055.4 according to OPS plus Na<sup>+</sup>, as shown in Figure 1. The structure was also identified by ATR-FTIR (cm<sup>-1</sup>): 3027 and 3071 (νC–H), 1595, 1432 (νC–C), 1088 (ν<sub>as</sub>Si–O–Si), 736,682 (ν<sub>s</sub>Si–O–Si); <sup>1</sup>H NMR (400 MHz, acetone): 7.398–7.830 ppm (H in phenyl group); solid <sup>29</sup>Si NMR (400 MHz): –74.4 ppm; The diameter of OPS particles is less than 400 nm according to SEM picture in Figure 2.

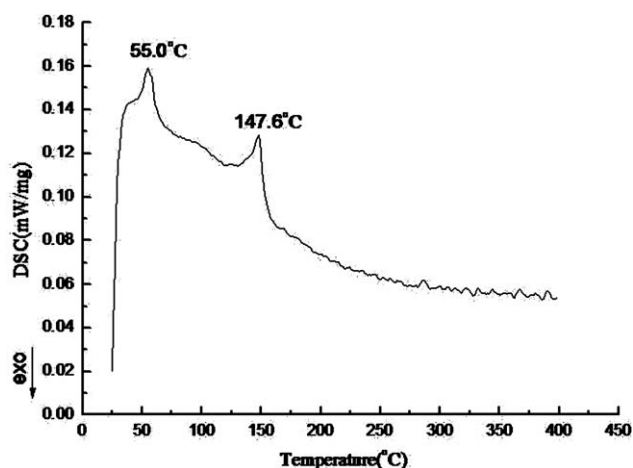
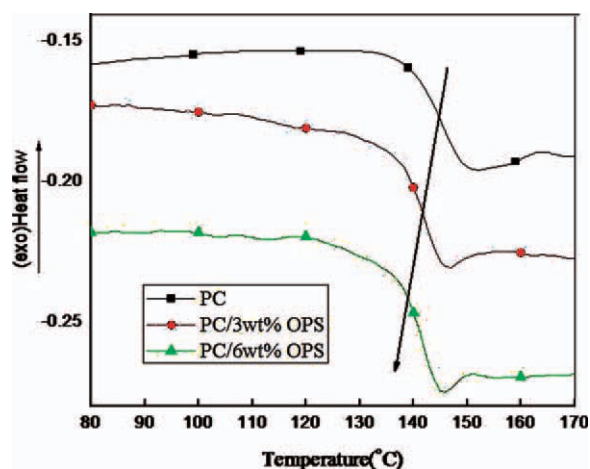


Figure 3 DSC curve of OPS compound Figure 3 DSC curve of OPS compound.



**Figure 4** DSC curves of PC and PC/OPS composites. [Color figure can be viewed in the online issue, which is available at [wileyonlinelibrary.com](http://wileyonlinelibrary.com).]

### Preparation of PC/OPS composites

Prior to blending, the PC pellets were dried for at least 5 h at 120°C in hot-air circulating oven. The composites were prepared blending PC and the different content of OPS, 0.3% PTFE, a small amount of antioxidant 1010 and 168 in the SJ-20 twin-screw extruder (screw diameter  $\Phi = 20$  mm; length to diameter,  $L/D = 40$ ). The screw temperature profile was set as 235, 240, 245, 245, 240, 230°C from the hopper to the die, and PC/OPS string was rapidly cooled in water and then pelletized. The PC/OPS pellets were dried and used in preparing different test samples by means of an Injection Molding Machine (HTF90X1, Haitian Plastics Machinery).

### Characterization

Differential scanning calorimeter (DSC) test

The calorimetry of the PC/OPS composites were performed on a Netzsch 204 F1 differential scanning calorimeter. Measurements were carried out under a continuous flow of nitrogen. About 5 mg sample was preheated at a scan rate of 10°C min<sup>-1</sup> from 40 to 180°C. Sample was cooled to ambient from the first scan and then scanned between 40 and 180°C and the thermograms were recorded at the scan rate of 10°C min<sup>-1</sup>. The glass transition temperature was taken as the midpoint of the capacity change.

**TABLE I**  
DMA and DSC Results for PC/OPS Composites

Samples	$E'$ at 30°C by DMA (GPa)	$T_g$ by DMA (°C)	$T_g$ by DSC (°C)
PC	1.19	148.6	145.1
PC/3 wt %OPS	1.58	141.6	141.2
PC/6 wt %OPS	1.64	140.3	139.9

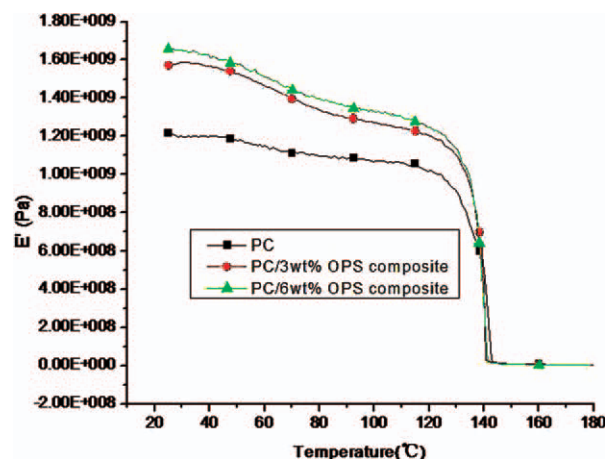


**Figure 5** Dynamic storage modulus of PC and PC/OPS composites. [Color figure can be viewed in the online issue, which is available at [wileyonlinelibrary.com](http://wileyonlinelibrary.com).]

Dynamic mechanical analysis (DMA) test

Dynamic mechanical analysis (DMA) measurements were performed in a N<sub>2</sub> atmosphere using a Rheometric Scientific DMTA V dynamic mechanical analyzer. The dimension of the specimens was 50 × 6 × 1.6 mm<sup>3</sup>. The measuring frequency was 1 Hz. The temperature was varied in the range 25–180°C at a heating rate of 3°C min<sup>-1</sup>.

Processing rheometer test

Processing rheology was studied using a Thermo-Haake Minilab Rheomex CTW5 laboratory-scale extruder (Thermo-Electron), with conical twin screws of 5–14 mm and a length of 109.5 mm. The Minilab had a maximum feed capacity of 6 g and for these experiments 5 g of PC and OPS was mixed. The processing torque of the melt was calculated automatically by the

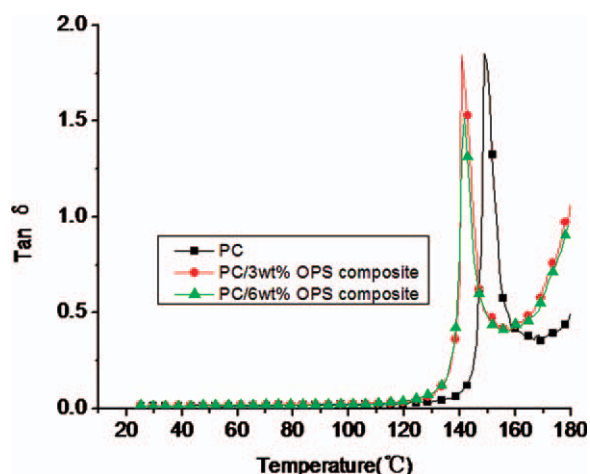


**Figure 6**  $\tan \delta$  of PC and PC/OPS composites. [Color figure can be viewed in the online issue, which is available at [wileyonlinelibrary.com](http://wileyonlinelibrary.com).]

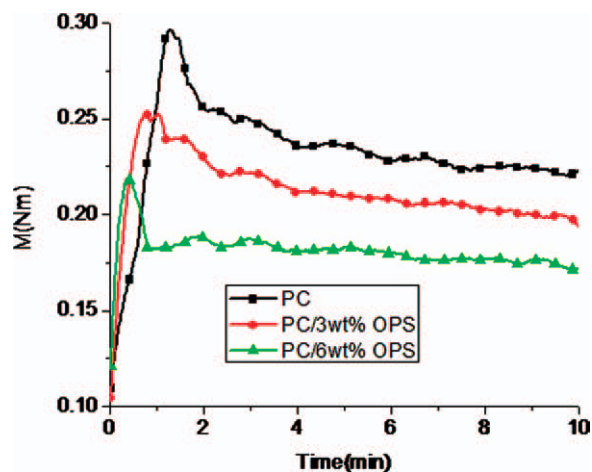


**Figure 7** Rheology curves of PC and PC/OPS composites (300°C). [Color figure can be viewed in the online issue, which is available at [wileyonlinelibrary.com](http://wileyonlinelibrary.com).]

Minilab by using the pressure difference between two pressure sensors located in the backflow channel.

#### Thermal gravimetric analysis (TGA)

Thermal gravimetric analysis (TGA) was performed on a Netzsch 209 F1 thermal analyzer at a heating rate of  $10^{\circ}\text{C min}^{-1}$  under  $\text{N}_2$  atmosphere, and the temperature ranged from 30 to  $800^{\circ}\text{C}$ . The onset thermal degradation temperature was taken as the temperature at which 5% mass loss occurred.

#### Scanning electron microscopy

Scanning electron microscopy (SEM) observation was performed with a Hitachi S-4800SEM to study the morphology of the PC/OPS composites and char residues. PC/OPS for SEM were prepared by low-temperature liquid nitrogen fracturing and sputtering the cross-section area with gold.

#### ATR-FTIR spectroscopy

IR spectra were recorded on a NICOLET 6700 IR spectrometer equipped with a Smart endurance single bounce ATR accessory. The spectra were collected in the spectral range  $4000\text{--}500\text{ cm}^{-1}$ , using 32 scans at  $4\text{ cm}^{-1}$  spectral resolution.

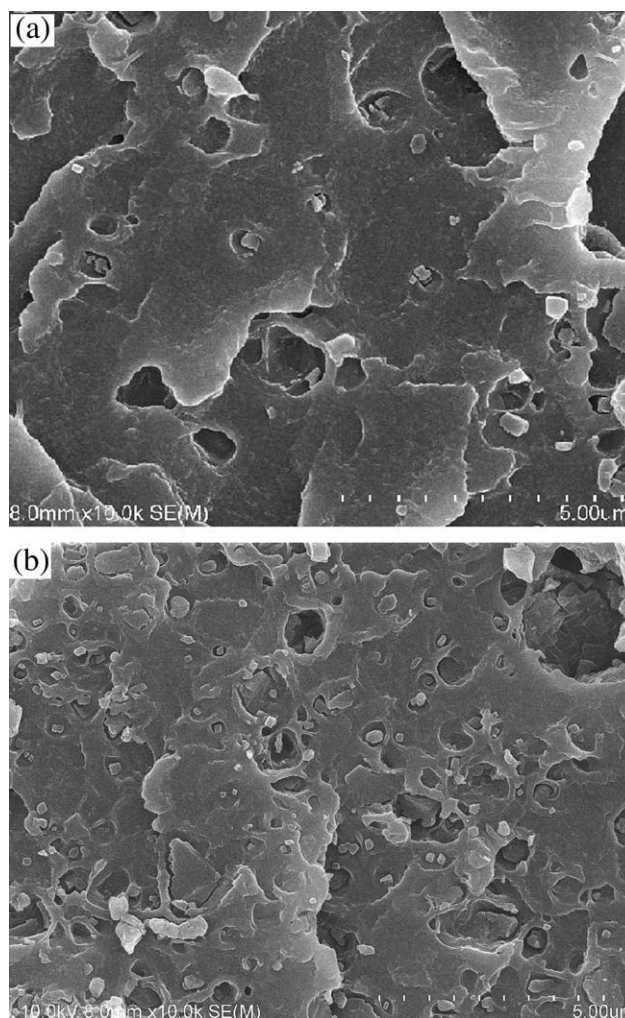


**Figure 8** SEM micrographs of PC/OPS composites: (a) PC/3 wt % OPS, (b) PC/6 wt % OPS.

#### Limiting oxygen index

Limiting oxygen index (LOI) measurement was carried out on a FTA-II instrument (Rheometric Scientific). The specimen dimension was  $130 \times 6.5 \times 3\text{ mm}^3$  according to ASTM D 2863-08 standard.

#### UL-94 vertical burning test

The UL-94 vertical burning measurements were performed on a CZF-3 instrument (Jiangning Analysis Instrument Factory). The specimen dimension was  $125 \times 12.5 \times 3.2\text{ mm}^3$  and  $125 \times 12.5 \times 1.6\text{ mm}^3$ .

**TABLE II**  
Mechanical Properties of PC and OPS/PC Composites

Samples	Tensile strength (MPa)	Elongation at break (%)	Elastic modulus (MPa)	Flexural strength (MPa)	Flexural modulus (MPa)	Notched Izod impact strength ( $\text{kJ m}^{-2}$ )
PC	63.3	102	1368	86.3	2392	11
PC/3 wt %OPS	61.4	81	1717	87.5	2464	–
PC/6 wt %OPS	59.3	64	1699	88.4	2544	15

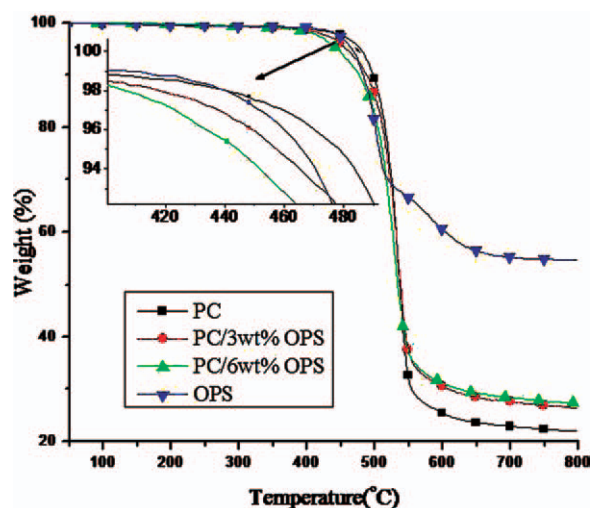


Figure 9 TGA curves of PC and PC/OPS composites. [Color figure can be viewed in the online issue, which is available at [wileyonlinelibrary.com](http://wileyonlinelibrary.com).]

#### Cone calorimeter test

Combustion experiments were performed on a cone calorimeter device (Fire Testing Technology) according to ISO-5660-1-2002 standard. Dimension of sample was  $100 \times 100 \times 3 \text{ mm}^3$  and the heat flux was  $50 \text{ kW m}^{-2}$ . The samples were wrapped in an aluminium foil leaving the upper surface exposed to the radiator and put the ceramic backing board at a distance of 25 mm from cone base. The results reported were the average of three replicated experiments.

## RESULTS AND DISCUSSION

### Thermal and dynamic mechanical analysis

In Figure 3, the DSC curve of OPS particle indicates it undergoes two phase transitions at 55.0 and

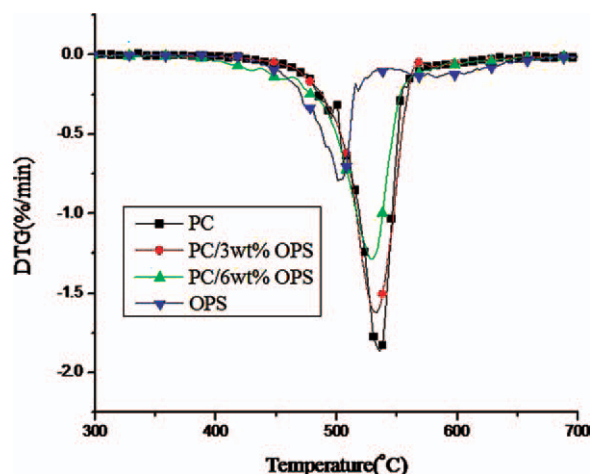


Figure 10 DTG curves of PC and PC/OPS composites. [Color figure can be viewed in the online issue, which is available at [wileyonlinelibrary.com](http://wileyonlinelibrary.com).]

TABLE III  
Thermogravimetric Parameters of OPS, PC, PC/OPS

Samples	$T_{\text{onset}}$ (°C)	$T_{\text{max}}$ (°C)	Residue at 800°C (%)
PC	478	535	22.0
OPS	465	501/572	54.6
PC/3 wt %OPS	457	532	26.6
PC/6 wt %OPS	445	529	27.4

147.6°C, respectively,<sup>21</sup> and has no obvious glass transition region. So during processing with PC the OPS was expected to be in a solid state. The DSC curves of PC and PC/OPS composites are presented in Figure 4. All the DSC thermograms displayed single glass transition temperature ( $T_g$ ) values in the experimental temperature range from 40 to 180°C. The  $T_g$  of PC/3 wt % OPS and PC/6 wt % OPS composite is lower than pure PC (145.1°C) in Figure 4 and Table I. The decrease in  $T_g$  could be ascribed to the non-molecular level dispersion of OPS on the PC matrix.

DMA of pure PC and PC/OPS composites were also evaluated as function of temperature. The curves of storage modulus  $E'$  and loss factor  $\tan \delta$  as are shown in Figures 5 and 6. The plateau  $E'$  values in the Table I before the glass transition are larger than that of the pure PC, suggesting that the OPS addition has a stronger influence on the dynamic modulus. The  $\tan \delta$  peaks of pure PC and PC/OPS composites displayed a well-defined relaxation peak in the temperature 40–180°C, which represents the glass–rubber transition of the polymer. The  $\tan \delta$  peak of the PC/OPS composites obviously shifts to a lower temperature than that of the corresponding pure PC, as one might expect for nonmolecular scale dispersion. The peak values of  $\tan \delta$  in Figure 6 show the PC/6 wt % OPS composite is lower than that of pure PC. The thermal glass transition temperature by DSC and the dynamic glass transition temperature by DMA are listed in Table I, which show almost the same decreasing trend.

In addition, the processing rheology of melt PC/OPS composites were tested by Minilab extruder. The curves of torque versus time are obtained as shown in Figure 7. It is found that the torque decreases with increasing OPS loading, which indicates that OPS particles help to decrease the viscosity of PC.

TABLE IV  
Flame Retardancy of PC and PC/OPS Composites

Samples	UL-94 (3.2 mm/1.6 mm)	LOI (%)
PC	V-2/NR	26.0
PC/3 wt %OPS	V-0/V-1	31.8
PC/6 wt %OPS	V-0/V-0	33.8

TABLE V  
Cone Calorimeter Parameters of PC and PC/OPS Composites

Samples	PC	PC/3 wt % OPS	PC/6 wt % OPS
TTI (s)	75	47	43
PHRR ( $\text{kJ m}^{-2}$ )	570	363	292
THR ( $\text{MJ m}^{-2}$ )	94.9	87.2	76.3
Mass loss (g)	32.9	31.8	22.9
mean CO ( $\text{kg kg}^{-1}$ )	0.151	0.105	0.008
mean CO <sub>2</sub> ( $\text{kg kg}^{-1}$ )	2.58	2.13	0.58

### Mechanical properties

The mechanical properties of PC/OPS composites were further investigated by tensile, flexural, and impact testing. The data are listed in Table II. The tensile strength of PC/OPS composites has a slight reduction; however, the elongation at break has a sharp decrease. This indicated that OPS have a poor compatibility with PC matrix. Oppositely, flexural strength and modulus increase monotonically with increasing OPS loading. Elastic modulus and impact strength of PC/OPS composites are higher than that of PC. The morphology of the PC/3 wt % OPS and PC/6 wt % OPS were further investigated by SEM. Figure 8 shows the SEM micrographs of the fractured surfaces of the composites frozen under cryogenic conditions using liquid nitrogen. The OPS containing composites exhibit a phase separation and OPS separates from with PC matrix. However, SEM micrographs on PC/OPS show a few aggregation either at 3 or 6 wt % OPS loading. The phase separation leads to the decrease of tensile strength and elongation at break. The reason of increase of modulus and flexible strength is probably an enhanced effect of ultrafine rigid OPS particles on PC.

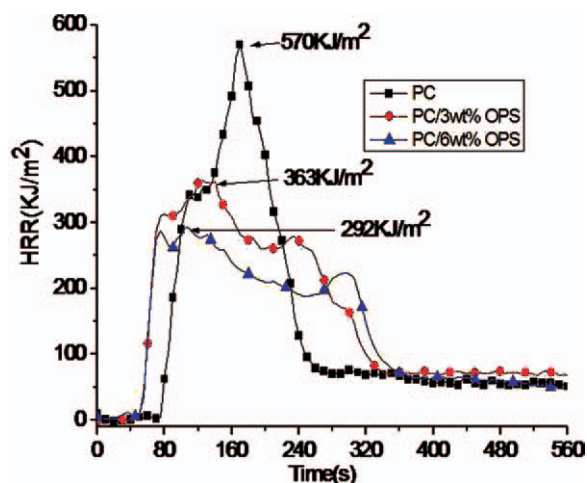


Figure 11 HRR curves of PC and PC/OPS composites. [Color figure can be viewed in the online issue, which is available at wileyonlinelibrary.com.]

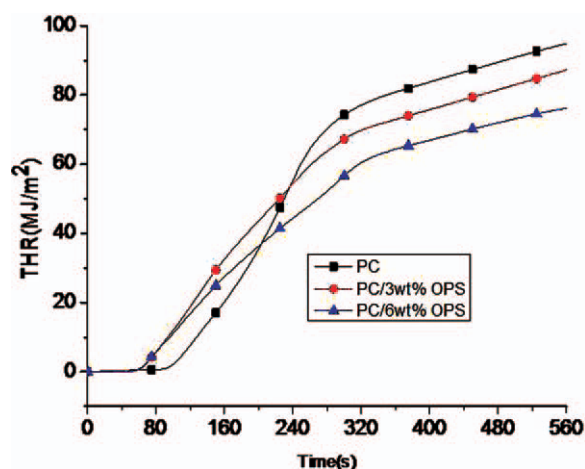


Figure 12 THR curves of PC and PC/OPS composites. [Color figure can be viewed in the online issue, which is available at wileyonlinelibrary.com.]

### Thermal stability

To investigate the effect of the OPS on the thermal stability and the decomposition behavior, TGA data under N<sub>2</sub> were determined and analyzed. TGA and DTG curves are presented in Figures 9 and 10. The relevant thermal decomposition data, including the  $T_{\text{onset}}$ , which is define as the temperature at which 5% weight loss occurs, the  $T_{\text{max}}$ , which is refer to as the temperature at maximum weight loss rate and the char residue at 800°C are listed in Table III.

Figure 9 shows that OPS had two weight loss processes, but PC and PC/OPS composites have a single weight loss process. The  $T_{\text{onset}}$  decrease from 478°C of PC to 445°C of PC/6 wt % OPS, suggesting OPS can accelerate the decomposition of PC. But the maximum decomposition temperature ( $T_{\text{max}}$ ) of PC and PC/OPS composites is very closely, as shown in Figure 10, it suggests that OPS has little affect by PC matrix. The presence of OPS didn't alter the thermal



Figure 13 Picture of char residue under cone calorimeter testing of PC. [Color figure can be viewed in the online issue, which is available at wileyonlinelibrary.com.]



**Figure 14** Picture of char residue under cone calorimeter testing of PC/6 wt % OPS composite. [Color figure can be viewed in the online issue, which is available at [wileyonlinelibrary.com](http://wileyonlinelibrary.com).]

behavior of PC nor its thermal degradation mechanism. Adding 6 wt % OPS to PC make the residue increase from 22 to 27.4%, indicating that OPS can make for char formation.

### Fire behavior

The LOI value describes a procedure for measuring the minimum concentration of oxygen that will just sup-

port flaming in a flowing mixture of oxygen and nitrogen. The UL-94 test is commonly used to determine the ignition resistance of materials. Table IV presents the LOI values and UL-94 testing results of PC and PC/OPS composites. As shown in Table IV, the LOI of PC is about 26.0%. The LOI value reach to 33.8% when the 6 wt % OPS was added into PC. At the same time, the UL-94 rating of the PC/3 wt % OPS composite could reach V-0 at 3.2 mm; the PC/6 wt % OPS composite could achieve V-0 at 1.6 mm without dripping. The result in UL-94 testing is different with previously PC/DOPO-POSS composites reported.<sup>22</sup>

The results of cone calorimeter test were summarized in Table V. The main parameters, such as time to ignition (TTI), heat release rate (HRR), total heat released (THR), mass loss, CO<sub>2</sub> and CO yield during combustion were obtained. As indicate in Table V, TTI of PC/6 wt % OPS composites are shorter than that of PC. This may be due to the initial decomposition temperature ( $T_{\text{onset}}$ ) of OPS is lower than that of PC, and OPS accelerate the thermal decomposition of PC matrix. It is reported that TGA can serve as useful indicators of polymer flammability in suitable circumstance.<sup>23,24</sup>

Figures 11 and 12 are the HRR curves and THR curves of PC and PC/6 wt % OPS composite independently. The peak heat release rate (PHRR) of PC/6 wt % OPS decrease from 570 kJ m<sup>-2</sup> of PC to 292 kJ m<sup>-2</sup>. HRR curve of PC is sharp, but that of PC/3 wt % OPS and PC/6 wt % OPS have two shoulder peak (Fig. 11). It indicated that OPS exists

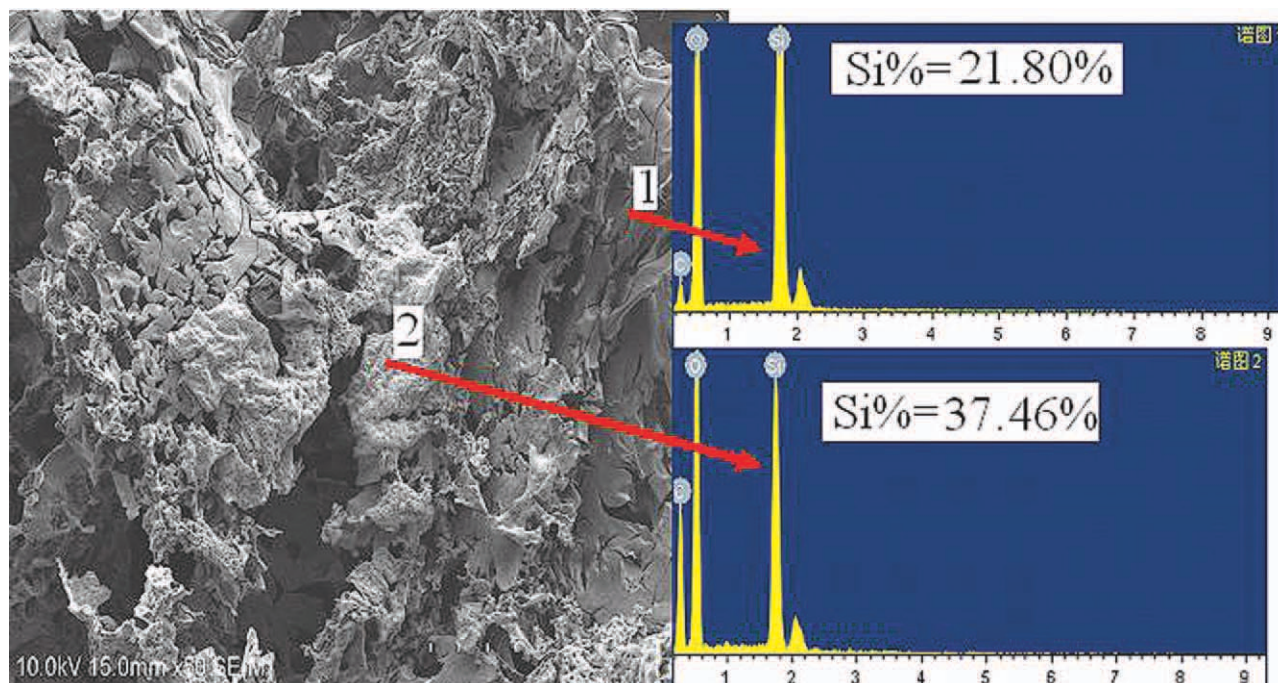


**Figure 15** SEM and EDS micrographs of PC/6 wt % OPS char residue. [Color figure can be viewed in the online issue, which is available at [wileyonlinelibrary.com](http://wileyonlinelibrary.com).]

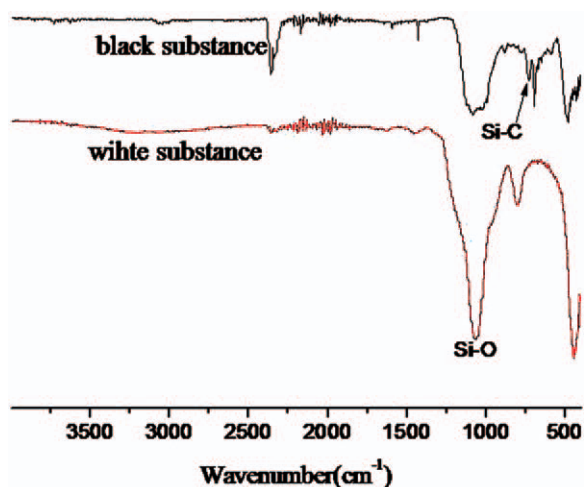


**Figure 16** ATR-FTIR spectrum of PC/6 wt % OPS char surface under cone calorimeter testing. [Color figure can be viewed in the online issue, which is available at [wileyonlinelibrary.com](http://wileyonlinelibrary.com).]

a process for the formation of char layer, resulting in a lower heat release rate. Furthermore, a decrease in mean carbon monoxide and dioxide are obtained. From Figure 10, it is observed that at the end of the test, THR of PC is  $103.4 \text{ MJ m}^{-2}$ , whereas, that of PC/6 wt % OPS composite is  $81.4 \text{ MJ m}^{-2}$ . These indicate that part of the composite has not been combusted completely. Mass loss of PC is more than that of PC/6 wt % OPS composite. During the PC/OPS composites combustion, the production of a lot of superficial ceramic layer led to the reduction of the mass loss. The ceramic layer acts as a physical protection by limiting heat transfer and mass transfer.

The pictures of char residue under cone calorimeter testing PC and PC/6 wt % OPS composite are presented in Figures 13 and 14. It is clear that the char of PC is less and more loose than that of PC/6 wt % OPS composite. There are many holes in the PC char so that it has collapsed after combustion ending. On the char surface of PC/6 wt % OPS the white substance is accumulated and the char is more compact than that of PC. From Figure 15, it is known the white substance is  $\text{SiO}_2$  which arises from the complete combustion of OPS.  $\text{SiO}_2$  aggregate are observed on the superficial char layer, and has a different weight percent, as confirmed by EDS analyses. The ATR-FTIR spectrum of the char of PC/6 wt % OPS in Figure 16 further confirm formation of the new Si-C bond during combustion.<sup>3</sup> However, the aggregate white substance in superficial char layer haven't been found in PC/DOPO-POSS systems previously reported.<sup>22</sup>

## CONCLUSIONS

PC/OPS composites have been prepared through direct melt blending. Both of DMA and DSC results showed that OPS decreased the glass transition temperature and increased of storage modulus of PC/OPS composites. PC/OPS composites displayed enhance in the flexural properties and impact strength. But tensile strength and elongation at break by mechanical testing were found to have a slight decrease. The OPS exhibit limited compatibility with PC matrix resulting in composites with a phase separation. TGA results showed that OPS accelerated the decomposition of PC. However, OPS didn't alter the thermal behavior of PC or its thermal degradation mechanism.

Highly flame retarded PC/OPS composites have been obtained by adding 6 wt % ultrafine OPS. The effect of OPS on the flame retarded PC is positive according to LOI value, UL-94 vertical burning rating and cone calorimeter results. When the OPS content was 6 wt%, the UL-94 rating reached V-0 at 1.6 mm, LOI value was 33.8% and the PHRR decreased from  $570$  to  $292 \text{ kJ m}^{-2}$ .

## References

- Jang, B. N.; Wilkie, C. A. *Thermochim Acta* 2005, 426, 73.
- Brunelle, D. J. *Advances in Polycarbonates*; American Chemical Society: Washington, DC, 2005; Chapter 1, p 1.
- Zhou, W.; Yang, H. *Thermochim Acta* 2007, 452, 43.
- Hayashida, K.; Ohtani, H.; Tsuge, S.; Nakanishi, K. *Polym Bull* 2002, 48, 483.
- Iji, M.; Serizawa, S. *Polym Adv Technol* 1998, 9, 593.
- Levchik, S. V.; Weil, E. D. *Polym Int* 2005, 54, 981.
- Hayashida, K.; Tsuge, S.; Ohtani, H. *Polymer* 2003, 44, 5611.
- Moore, S. *Mod Plast* 1998, 75, 35.
- Zhou, W. J.; Yang, H.; Zhou, J. *J Anal Appl Pyrol* 2007, 78, 413.
- Masatoshi, I.; Shin S. *Polym Adv Technol* 1998, 9, 593.
- Fina, A.; Tabuani, D.; Camino, G. *Eur Polym J* 2010, 46, 14.
- Fina, A.; Abbenhuis, H. C. L.; Tabuani, D.; Camino, G. *Polym Degrad Stab* 2006, 91, 2275.
- Sanchez-Soto, M.; Illescas, S.; Milliman, H.; Schiraldi, D. A.; Arostegui, A. *Macromol Mater Eng* 2010, 295, 846.
- Zhou, Z. Y.; Zhang, Y.; Zeng, Z.; Zhang, Y. X. *J Appl Polym Sci* 2008, 110, 3745.
- Song, L.; He, Q. L.; Hu, Y.; Chen, H.; Liu, L. *Polym Degrad Stab* 2008, 93, 627.
- Zhao, Y. Q.; Schiraldi, D. A. *Polymer* 2005, 46, 11640.
- Sanchez-Soto, M.; Schiraldi, D. A.; Illescas, S. *Eur Polym J* 2009, 45, 341.
- Nagendiran, S.; Alagar, M.; Hamerton, I. *Acta Mater* 2010, 58, 3345.
- Vlrich, S.; Nicola, H. S.; Richard, M. L. *Materials Syntheses: A Practical Guide*; Springer Wien: NewYork, 2008; p 179.
- Brown, J.; Vogt, L.; Prescott, P. *J Am Chem Soc* 1964, 86, 1120.
- Larsson, K. *Arkiv Kemi* 1960, 16, 209.
- Zhang, W. C.; Li, X. M.; Guo, X. Y.; Yang, R. J. *Polym Degrad Stab* 2010, 95, 2541.
- Cullis, C. F.; Hirschler, M. M. *Polymer* 1983, 24, 834.
- Hirschler, M. M. *Eur Polym J* 1983, 19, 121.